



HAL
open science

Multi-Task Architecture with Attention for Imaging Atmospheric Cherenkov Telescope Data Analysis

Mikaël Jacquemont, Thomas Vuillaume, A Benoit, Gilles Maurin, Patrick Lambert

► **To cite this version:**

Mikaël Jacquemont, Thomas Vuillaume, A Benoit, Gilles Maurin, Patrick Lambert. Multi-Task Architecture with Attention for Imaging Atmospheric Cherenkov Telescope Data Analysis. VISAPP 2021, Feb 2021, online, France. hal-03043188

HAL Id: hal-03043188






<https://hal.science/hal-03043188v1>

Submitted on 4 Feb 2021

HAL is a multi-disciplinary open access archive for the deposit and dissemination of scientific research documents, whether they are published or not. The documents may come from teaching and research institutions in France or abroad, or from public or private research centers.

L'archive ouverte pluridisciplinaire **HAL**, est destinée au dépôt et à la diffusion de documents scientifiques de niveau recherche, publiés ou non, émanant des établissements d'enseignement et de recherche français ou étrangers, des laboratoires publics ou privés.

Multi-Task Architecture with Attention for Imaging Atmospheric Cherenkov Telescope Data Analysis

Mikaël Jacquemont^{1,2}^a, Thomas Vuillaume¹^b, Alexandre Benoit²^c, Gilles Maurin¹^d, Patrick Lambert²^e

¹*CNRS, LAPP, Univ. Grenoble Alpes, Université Savoie Mont Blanc, Annecy, France*

²*LISTIC, Univ. Savoie Mont Blanc, Annecy, France*
{jacquemont,vuillaume}@lapp.in2p3.fr

Keywords: multitasking, artificial neural networks, gamma rays, attention

Abstract: Gamma-ray reconstruction from Cherenkov telescope data is multi-task by nature in astrophysics. The image recorded in the Cherenkov camera pixels relates to the type, energy, incoming direction and distance of a particle from a telescope observation. We propose γ -PhysNet, a physically inspired multi-task deep neural network for gamma/proton particle classification, and gamma energy and direction reconstruction. We compare its performance with single task networks on Monte Carlo simulated data and demonstrate the interest of reconstructing the impact point as an auxiliary task. We also show that γ -PhysNet outperforms a widespread analysis method for gamma-ray reconstruction. Finally, we study attention methods to solve relevant use cases. All the experiments are conducted in the context of single telescope analysis for the Cherenkov Telescope Array data analysis.

1 INTRODUCTION

Gamma-ray astronomy is the astronomical observation of the most energetic photons (above 100 keV) produced by violent astrophysical phenomena (supernova remnants, gamma-ray bursts, active galactic nuclei, etc.) and potentially by dark matter annihilation.

When these high-energy particles enter the atmosphere, they interact with its dense matter producing a particle shower. As illustrated in Figure 1, Imaging Atmospheric Cherenkov Telescopes (IACTs) observe the Cherenkov radiation (Hillas, 1985) emitted by this shower. Their large mirrors collect the light to form an image recorded by a high sensitivity camera usually made of photomultipliers. The gamma shower then appears as an ellipsoid.

Since the first IACT, the Whipple observatory constructed in 1968, many others have been built (e.g., H.E.S.S., MAGIC or VERITAS), mainly as arrays of telescopes to make the most of the stereoscopic techniques. The Cherenkov Telescope Ar-

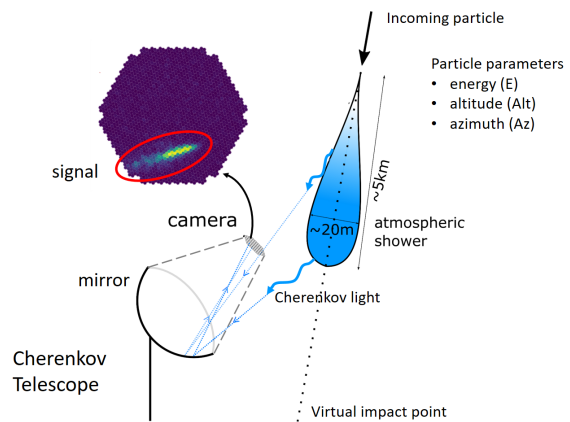






Figure 1: Imaging Atmospheric Cherenkov Telescope


ray (CTA), the next generation of IACTs, will improve sensitivity by a factor of 10 while also increasing accuracy in gamma-ray detection. To achieve these improvements, CTA will be composed of ~ 100 telescopes of three different sizes with very high-speed cameras (telescope readout event rate in kHz range[0.6, 10]). When in full operation, CTA will produce 210 PB of raw data per year to be analyzed in real time and then reduced and compressed to 3 PB before archiving. Moreover, thanks to an improving knowledge of the telescopes and thus better analysis

^a <https://orcid.org/0000-0002-4012-6930>

^b <https://orcid.org/0000-0002-5686-2078>

^c <https://orcid.org/0000-0002-0627-4948>

^d <https://orcid.org/0000-0002-6970-0588>

^e <https://orcid.org/0000-0003-0478-9443>

algorithms, all the data already acquired will be re-processed every year.

The Large Size Telescope 1 (LST1 (Ambrosi et al., 2013)) is the first prototype installed at the Northern CTA site in La Palma. It has been designed to detect gamma rays with an energy between 30 GeV and 3 TeV, which is especially interesting for the study of transient phenomena such as gamma-ray bursts recently observed for the first time by IACTs (Abdalla et al., 2019). During this preparation phase, analysis methodologies are developed on simulated data that make method comparison possible.

The purpose of the image analysis is to estimate the energy and direction (as altitude and azimuth) of the primary particle and to separate the gamma rays from the cosmic ray background, mainly composed of protons. This step is complex because cosmic rays can generate very similar images and the signal-to-noise ratio is typically lower than 1/1000. The analysis method is then driven by the gamma detection in a high background noise and the regression of its parameters in big data context. Moreover a sensitive and real-time reconstruction will allow tracking and discovering new astrophysical phenomena.

Several approaches have been considered in the past to perform this analysis. The most common was developed by A. M. Hillas (Hillas, 1985). It characterizes the ellipsoid image by its moments up to second order. To improve the sensitivity, these parameters have been combined with multivariate analysis methods, relying on boosted decision trees or random forests (Fiasson et al., 2010). Such approach will next be referred to as Hillas + RF. However, this approach doesn't take into account the strong interdependence between the energy, the arrival direction, the virtual impact point on the ground of the particle and the image produced (i.e., pixel intensity, shower shape and position) that make the reconstruction multi-task by nature. State-of-the-art methods (de Naurois and Roland, 2009), named Template analysis, are based on a pixel level comparison relying on a likelihood between a bank of image templates and the recorded images. However, they are very slow (Parsons et al., 2016) and each telescope of the array needs a huge database of templates, which is not tractable for CTA real-time analysis.

In this paper, we propose a deep multi-task architecture, named γ -PhysNet, for single telescope gamma event reconstruction (i.e., **gamma/proton classification, energy and arrival direction reconstruction**) from IACT simulated data. Based on Convolutional Neural Networks (CNNs), the proposed model has an inference rate close to the LST1 acquisition rate, above 2.5kHz. We demonstrate the in-

terest of multi-task learning for IACT data analysis and show that our architecture outperforms the widespread Hillas + RF analysis method, in particular on direction reconstruction and gamma/proton classification that are critical to improve the sensitivity of the telescope. We then study several attention mechanisms for the proposed architecture in two different configurations to address relevant use cases.

2 RELATED WORK

2.1 Deep Learning for Imaging Atmospheric Cherenkov Telescope Data

Over the past decade, deep learning has emerged as the leading approach in many computer vision tasks, including image classification (Touvron et al., 2019), semantic segmentation (Yuan et al., 2020) and object detection (Zhang et al., 2020). Recently, some effort has been made to explore deep learning techniques to solve astrophysical problems (Kim and Brunner, 2016; Brunel et al., 2019). IACT data analysis isn't out of step, from muon image analysis (Feng et al., 2016) to gamma event reconstruction of CTA data or other IACTs. Nieto *et al.* (Nieto et al., 2017) probe very deep networks for gamma/proton classification. Reference (Mangano et al., 2018) presents a narrower CNN to solve gamma/proton classification, and energy and direction regression tasks. Shilon *et al.* (Shilon et al., 2019) propose a combination of a CNN and a Recurrent Neural Network, denoted CRNN, to solve the same tasks in stereo-analysis (using several telescopes). To solve the real data discrepancy issue, Parsons *et al.* (Parsons and Ohm, 2019) propose to combine IACT images and standard method parameters. These papers present promising results, especially for gamma/proton classification. However, they have handled the different reconstruction problems as single tasks, without considering their strong interdependence.

2.2 Multi-task learning

Multi-task learning (MTL) is a learning paradigm which aims to improve the generalization (Caruana, 1997) of learned models. Former approaches (Thrun, 1996) have shown that transferring knowledge across related tasks improves the generalization with fewer data. MTL helps the model focus on features that are relevant for all tasks. Recent methods based on

CNN have shown remarkable results on pose estimation (Pavlo et al., 2019) or instance segmentation (He et al., 2017).

In MTL, the tasks to address are trained simultaneously, using a partially shared representation. In hard parameter sharing architectures, the most frequently used, a whole part of the network is shared between all tasks (Ruder, 2017). The shared part is generally the encoder (Luvizon et al., 2018) or its first layers (Iizuka et al., 2016). In soft parameter sharing architectures (Cao et al., 2018), each task is learned with its own network. However, some additional layers are shared and constrained in order to encourage their weights to be similar.

Balancing the tasks is critical. For most of the MTL related papers (Luvizon et al., 2018; Ren and Jae Lee, 2018), this is done, when specified, by hand. This handcrafted weighting needs an extensive optimization process to find optimal ones. However, adaptive methods have been proposed in order to automatically balance task importance. Kendall *et al.* (Kendall et al., 2018) model the homoscedastic uncertainty for each task and use it as a proxy for task balancing. Reference (Chen et al., 2018) proposes to weight the tasks in order to balance their loss gradient with regard to the last common layer. This leads to penalizing predominant tasks and encouraging weaker tasks. Guo *et al.* (Guo et al., 2018) use learning progress signals as key performance indicators to prioritize difficult cases at both task and example level. Sener *et al.* (Sener and Koltun, 2018) consider MTL as a multi-objective optimization to achieve Pareto optimality for each task scale factor.

In this work, we propose a hard parameter sharing architecture. Besides, to balance the tasks the Kendall approach proved to be the most relevant.

2.3 Attention in Deep Learning

Attention is a mechanism that helps deep learning model focus on relevant features based on a defined context through trainable weights. It originates from the natural language processing (NLP) field (Bahdanau et al., 2015) and is the main component of Transformer networks (Vaswani et al., 2017) that achieve state-of-the-art performance on neural machine translation and image captioning. Parmar *et al.* (Parmar et al., 2018) generalize the Transformer architecture to image generation. Restricted self-attention is considered to focus on local neighborhoods. On the other hand, Wang *et al.* propose global self-attention as a non-local operation for video classification, image segmentation, object detection and pose estimation (Wang et al., 2018). Zhang *et al.*

(Zhang et al., 2019) adapt the global self-attention for generative adversarial networks (GANs). They use a stronger bottleneck controlled by a factor k , denoted reduction ratio in the following. In addition, they introduce a learnable parameter to scale the output of the attention module before summing back with the input. While for computer vision tasks attention modules are generally combined with convolution blocks, Ramachandran *et al.* (Parmar et al., 2019) propose stand-alone local self-attention models for image classification and object detection.

Global and local self-attention can be considered as spatial attention mechanisms, as they capture long-range dependencies in data, by weighting each pixel. On the contrary, Hu *et al.* (Hu et al., 2018) introduce a lightweight channel-wise attention denoted Squeeze-and-Excitation. The squeeze operation produces a channel descriptor of the input and is followed by an adaptive recalibration, the excitation, and a scale operation that weights the input channels. The excitation acts as a bottleneck parametrized by a reduction ratio. Reference (Sun et al., 2020) proposes dual attention for U-Net to help improve model interpretability and robustness. It combines Squeeze-and-Excitation with a simple spatial attention path. The latter compresses the number of input channels to one. It then applies a sigmoid to the resulting pixel values to produce an attention map that rescales the output of the Squeeze-and-Excitation.

In this paper, we compare self-attention, Squeeze-and-Excitation and Dual Attention.

3 γ -PHYSNET FOR FULL EVENT RECONSTRUCTION

3.1 Multi-task Architecture

We propose a MTL architecture, γ -PhysNet, to achieve full event reconstruction from IACT data. As computation time is crucial, this is a hard parameter sharing architecture composed of a backbone encoder and a physically inspired multi-task block. The network is fed with two-channel IACT data (see Section 4.1 for details) and, in a single pass, separates gamma rays from background noise, and reconstructs the energy and the arrival direction of the primary particle. It benefits from the regression of the virtual impact point of the particle as an auxiliary task. Even though it is not needed by astronomers for higher-level analysis, physics shows that this parameter provides meaningful information to solve energy and direction reconstruction tasks.

Relying on an extensive ablation study that we cannot report in this paper, the backbone of γ -PhysNet is the convolutional part of a ResNet-56 (He et al., 2016b; He et al., 2016a), CIFAR-10 version, with full pre-activation implemented with IndexedConv (Jacquemont et al., 2019). IACT images can have hexagonal pixels, as is the case for the LST cameras. As there is no clear advantage so far (Nieto et al., 2019) to transform them to square pixel images in terms of performance, indexed convolutions provided by IndexedConv package make it possible to process directly hexagonal images.

The specificity of γ -PhysNet lies in its physically inspired multi-task block. As illustrated in Figure 2, it is composed of a global feature network and a local feature network, both made of fully connected layers. The global feature part, starting with a global average pooling, is dedicated to energy regression as energy can be considered as a global parameter with regard to the input images: for a given arrival direction and impact point, the amplitude of the acquired image is roughly proportional to the primary gamma ray energy (Völk and Bernlöhr, 2009). The local feature part is fed with flattened feature maps provided by the backbone encoder. It intends to exploit local and spatial information to solve gamma/proton classification, and arrival direction and impact point regression tasks as these reconstructed parameters are more deeply related to the shape, position and orientation of the signal in the camera.

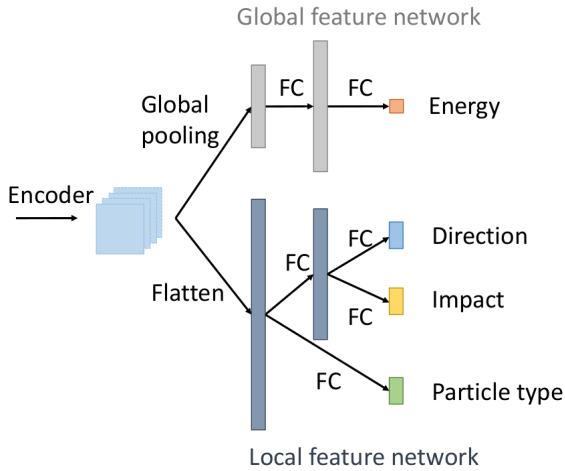


Figure 2: Physically inspired Multi-task block.

3.2 Augmenting the Backbone with Attention

The backbone of γ -PhysNet is composed of an initial convolution and three stages of nine residual blocks

each. The first layer of every stage is a subsampling performed with a strided convolution. As illustrated in Figure 3, we insert the attention modules after every stage to benefit from attention at each feature size scale. Note that, in order to be compliant with our case study, attention modules are not inserted into backbone stages in order to limit the model complexity and processing cost increase.

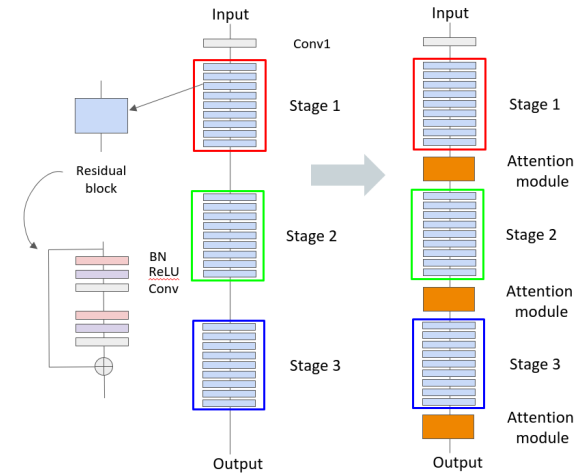


Figure 3: Adding attention to γ -PhysNet backbone. We insert the attention modules after every stage of the ResNet-56.

In this paper, we focus on Squeeze-and-Excitation (SE), self-attention (SA) and dual attention (DA).

3.3 Computational Cost

The whole network, implemented with PyTorch, has 2.6×10^6 parameters (for LST images). Although it has not yet been optimized for production, γ -PhysNet inference rate on an NVIDIA V100 GPU is similar to the telescope acquisition rate, from 2.5 to 4.5 kHz depending on the attention method.

4 EXPERIMENTS

We first demonstrate the interest of multi-task learning for IACT data analysis on simulated data for CTA. We also show that the proposed architecture outperforms a widespread analysis method. Then we study attention mechanisms for γ -PhysNet backbone with two data filtering configurations to address different analysis use cases.

4.1 Dataset

For the following experiments, we use the dataset referenced as the LST4 mono-trigger Production (from 2019/04/15), the large-scale Monte Carlo production generated by the LST collaboration for the LST1 commissioning. This dataset is not yet publicly available. The specificity of this production is that it only contains the data of the four LSTs of the Northern site of CTA. It is composed of events of different types, including diffuse gammas, gammas from point sources (dubbed as *point-like*) and protons. Diffuse events correspond to extended sources while *point-like* events correspond to sources situated at a particular direction. Gammas and protons have different simulated energy distributions, both following a power law with a spectral index of -2, leading to an imbalanced dataset in terms of number of events per energy.

The dataset has been calibrated and integrated with DL1DataHandler (Kim et al., 2019). It is separated into a training set and a test set for each event type. The images have two channels, one for pixel intensity (unit being the number of photoelectrons) and the other containing per-pixel temporal information (time delays from the beginning of the event recorded by the telescope). Data amplitude is not normalized since it is related to the energy of the detected particles (Völk and Bernlöhr, 2009). Again, we rely on simulated data as ground truth is impossible to obtain from real data, and real CTA data are not yet available. Moreover, it allows for an in-depth comparison of the models.

4.2 Training

For the following experiments, we train all the models using the data from the four telescopes of this LST4 mono-trigger dataset to provide a more accurate overview of the data variability. The models are trained on gamma diffuse events, so as to reconstruct events coming from any directions within the field of view, and on proton events.

For reproducibility, we repeat the experiments for all the probed configurations with six different random seeds for parameter initialization. We use the standard cross-entropy loss for the classification task and the $L1$ loss for regression tasks. All the neural networks are trained with the same hyperparameters. Indeed, a single experiment typically requires between 4 and 40 hours (depending on the data selection) on a V100 GPU hardware. Consequently, an advanced optimization study of all the compared networks is not feasible at the step of the project. How-

ever, starting from the default optimized hyperparameters of ResNet, extensive preliminary experiments allowed defining a common and well-performing hyperparameter set. We train the models for 25 epochs with Adam (Kingma and Ba, 2015) as the optimizer. The learning rate is set to 10^{-3} and is decayed by a factor of 10 every 10 epochs. We regularize the networks by applying a $L2$ penalty with a weight decay of 10^{-4} on their weights. We balance the different tasks with the uncertainty estimation method presented in (Kendall et al., 2018). The task weights are also learned with Adam as the optimizer with a learning rate of 0.025 and a weight decay of 10^{-4} . In gamma-ray astronomy, proton events are considered as background noise. To prevent them from disturbing the learning of energy and direction task for gamma events, we rely on a masked loss method. We set to zero the loss of the regression parameters (energy, arrival direction and impact point) when particles are protons.

4.3 Evaluation Metrics

To comply with gamma-ray astronomy standardized practice and most common scientific use cases, we evaluate the different configurations on gamma *point-like* and proton events. Their performance on energy and direction reconstruction tasks is measured through resolution curves. The energy resolution represents, per energy bin, the half-width of the interval around 0 which contains 68% of the distribution of the relative prediction error. The angular resolution represents, per energy bin, the angle within which 68% of reconstructed gamma rays fall, relative to their true direction. For both, lower is better. For the gamma/proton classification task, the overall performance of the network is given by the area under the ROC curve (AUC) and the F1 score.

As we repeat the experiment six times for all the models, we illustrate the variability of these different runs by drawing the resolution curves as surfaces, referred to as dispersion in this paper. The envelope of the surface represents the min / max per bin and the dots represent the average resolution per bin of the six random seeds. This "average" resolution is not related to any physical reality as resolution is a statistical measure of the error of a particular model. However, it gives a trend of the model performance and is useful for readability.

4.4 Multi-task Learning Performance

In this section we evaluate the interest of multi-task learning for IACT data analysis, i.e., gamma/proton

classification, energy and direction regression. We compare the proposed architecture with single task networks (ResNet-56). We probe the importance of the impact point regression as an auxiliary task by training γ -PhysNet without the impact point task (γ -PhysNet w/o impact). We compare with a widespread analysis method for IACTs event reconstruction (Hillas + RF). The toolchain used, designed relying on the open-source library cta-1stchain v0.1.0, consists in extracting relevant image features followed by inferring target particle parameters with random forests using the library scikit-learn (Pedregosa et al., 2011).

In this paper we cannot compare with (Shilon et al., 2019) and (Mangano et al., 2018) as the architectures presented are designed for stereo analysis while our architecture is designed for single telescope analysis. We neither compare with (Nieto et al., 2017) as this work is related to a different telescope, is focused on classification and does not take into account the temporal information.

A series of selection cuts on image amplitude, shower size and truncated showers is applied to the data in order to keep good quality events. These cuts are standard in the domain and necessary for the comparison with Hillas + RF method that discards the bad quality events. The training set is composed of 388k gamma diffuse events and 236k proton events.

4.4.1 Gamma/Proton Classification

Table 1 clearly shows that our model outperforms the Hillas + RF analysis method in both AUC and F1 score. More specifically, the proposed architecture improves the AUC by 6.9% and the F1 score by 30.7% compared to Hillas + RF. The contribution of multitasking in γ -PhysNet architecture is also significant compared to the single task approach relying on the ResNet architecture. However, the benefit of the impact point regression as an auxiliary task is not obvious for gamma/proton classification.

Table 1: AUC and F1 score of the gamma/proton classification task for the different models

Model	AUC	F1 score
Hillas + RF	0.898	0.732
ResNet-56	0.954 \pm 0.001	0.949 \pm 0.001
γ -PhysNet	0.960\pm0.002	0.956\pm0.002
γ -PhysNet w/o Impact	0.961\pm0.002	0.955\pm0.001

4.4.2 Energy Reconstruction

Figure 4 shows that all the evaluated deep neural networks (DNNs) outperform the Hillas + RF method for the energy reconstruction task. γ -PhysNet decreases the relative error on the energy task by up to 0.08 at high energies and up to 1.1 at 31 GeV (the point of the Hillas + RF curve is out of the plot). The resolution curves of γ -PhysNet and the ResNet-56 are very close almost everywhere. However γ -PhysNet has slightly better results below 200 GeV. At energies above 400 GeV, MTL seems to degrade the performance, in particular without the regression of the impact point. This can be explained physically as the particle energy is strongly correlated with the observed intensity in the camera and the distance from the telescope to the shower impact point. MTL models have a higher dispersion than the single task model.

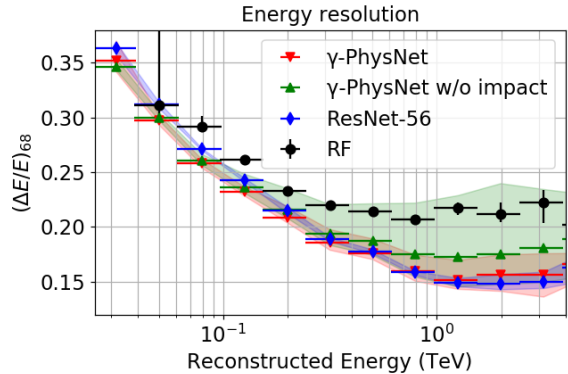


Figure 4: Energy resolution as a function of the energy in the LST energy range (lower is better). Comparison of the performance on the energy regression task between the probed models.

4.4.3 Direction Reconstruction

As for the gamma/proton classification and the energy regression tasks, Figure 5 shows that DNNs outperform the Hillas + RF analysis method for the direction reconstruction task. In particular, γ -PhysNet improves the performance by 0.03° to 0.3° compared to Hillas + RF. Moreover, for this task the contribution of MTL is significant, improving the results by up to 0.08° compared to the single task network. The proposed architecture has also slightly better results with the impact point reconstruction as an auxiliary task, especially at higher energies (> 1 TeV). Both MTL models have a lower variability.

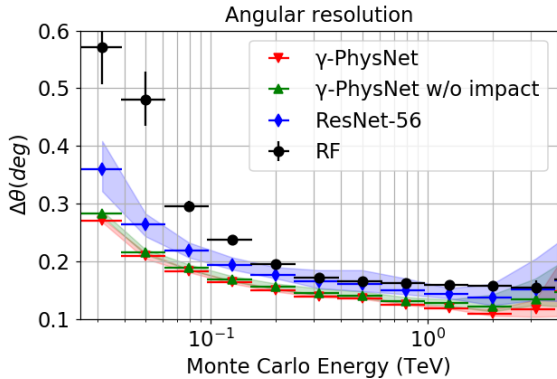


Figure 5: Angular resolution as a function of the energy in the LST energy range (lower is better). Comparison of the performance on the arrival direction regression task between the probed models.

4.5 Impact of the Attention Mechanisms

Our experiments presented in Section 4.4 show that the proposed architecture outperforms the widespread Hillas + RF analysis method and that MTL improves the performance, especially for the direction reconstruction task. In this section we focus on attention mechanisms for the backbone of γ -PhysNet. We evaluate the different configurations (γ -PhysNet, γ -PhysNet SE, γ -PhysNet SA and γ -PhysNet DA) presented in Section 3.2 on the same data. To address relevant use cases in gamma astronomy, we investigate two series of selection cuts on image amplitude and truncated showers, denoted high cuts (HC) and low cuts (LC). These are different from Section 4.4 as we don't compare with Hillas + RF.

The HC consists in selecting images whose total amplitude is higher than 1,000 photoelectrons while higher than 50 photoelectrons for the LC. For both we keep events whose shower is more than 80% contained in the camera frame.

The HC is highly selective (training set: 121k gammas and 75k protons), mainly at the lowest energies. The remaining events contain well defined and bright showers. In the context of single telescope analysis, their parameters are easier to reconstruct, in particular their arrival direction. Models trained with the HC can address the use case of morphological study of extended and bright sources.

The LC is far less selective (training set: 874k gammas and 506k protons). It is worth noticing that it is also less selective than the standard cuts applied in Section 4.4. It allows processing more events of lower energy albeit of less good quality. Models trained with the LC can possibly address three use cases. We can analyze sources emitting photons with en-

ergy lower than 100 GeV. This is particularly relevant to the study of extragalactic objects and gamma-ray bursts. As a second use case, we can observe the temporal variability of the flux of well-known sources. Finally, we can also realize sky surveys to discover new sources.

As detailed in Section 2.3, the probed attention methods have a hyperparameter to control their bottleneck, denoted reduction ratio. Relying on an extensive ablation study, we use the reduction ratio presented in Table 2 for the three attention mechanisms and the two selection cuts. Noteworthy, depending on the selection cuts we apply, the best reduction ratio per attention mechanisms varies.

Table 2: Selected reduction ratio for the three attention methods and the two selection cuts.

Attention	HC	LC
Squeeze-and-Excitation	2	4
Self-Attention	12	12
Dual Attention	8	16

4.5.1 High Cuts

Table 3 shows that all three attention methods and the model without attention have similar results on the classification task. For the energy and direction regression, Figure 6 and Figure 7 present the results of the different methods in the range 100 GeV to 3 TeV as the selection filters discard most events below 100 GeV. On the energy reconstruction task, all the attention methods probed have a better average performance than the model without attention. Their results are also less spread. In particular, the dual attention mechanisms performs clearly better on average, improving the resolution up to 0.055. Its dispersion is four times smaller than the one of self-attention. The model without attention spreads ten times more. On the direction reconstruction task, γ -PhysNet with the Squeeze-and-Excitation and the dual attention mechanisms outperform the other models, in average performance and in dispersion. In particular, they improve the resolution by 0.02° on most of the energy range of interest, achieving a resolution of 0.1° with a dispersion of 0.01°.

4.5.2 Low Cuts

With the low cuts, γ -PhysNet with the self-attention method performs slightly worse on the classification task, as shown in Table 4. The other models have comparable results within the standard deviation range. For the energy and direction regression, Figure

Table 3: High Cuts. AUC and F1 score of the gamma/proton classification task for the different models.

Model	AUC	F1 score
γ -PhysNet	0.990 ± 0.001	0.981 ± 0.001
γ -PhysNet SE[2]	0.991 ± 0.001	0.981 ± 0.000
γ -PhysNet SA[12]	0.989 ± 0.001	0.980 ± 0.001
γ -PhysNet DA[8]	0.991 ± 0.001	0.982 ± 0.001

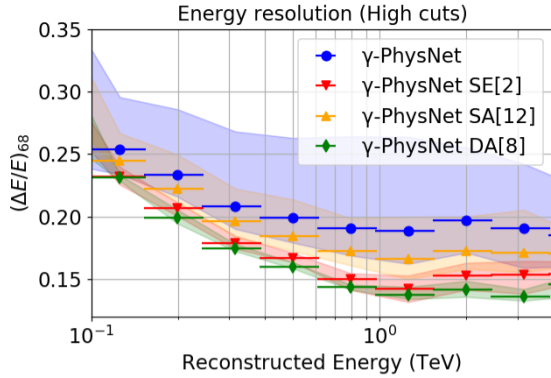


Figure 6: High cuts. Energy resolution as a function of reconstructed energy. Comparison of the different attention mechanisms for γ -PhysNet. The surface represents the min / max envelope per bin and the dots represent the average resolution per bin of the six seeds.

8 and Figure 9 present the results in the same energy range as for the high cuts for easy comparison. Moreover, below 100 GeV all models have similar performance on both tasks. On the energy reconstruction task, the models with Squeeze-and-Excitation and dual attention perform better. They improve the re-

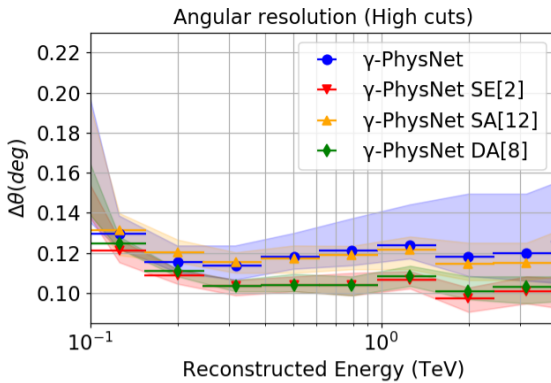


Figure 7: High cuts. Angular resolution as a function of reconstructed energy. Comparison of the different attention mechanisms for γ -PhysNet. The surface represents the min / max envelope per bin and the dots represent the average resolution per bin of the six seeds.

sults up to 0.03, in particular at high energies. All the networks with attention have significantly less spread results. On the direction reconstruction task, again the models with Squeeze-and-Excitation and dual attention have better performance, improving the resolution up to 0.02° . All the models have similar dispersion in their results.

Table 4: Low Cuts. AUC and F1 score of the gamma/proton classification task for the different models.

Model	AUC	F1 score
γ -PhysNet	0.882 ± 0.001	0.932 ± 0.003
γ -PhysNet SE[4]	0.883 ± 0.002	0.931 ± 0.002
γ -PhysNet SA[12]	0.879 ± 0.003	0.930 ± 0.001
γ -PhysNet DA[16]	0.882 ± 0.001	0.932 ± 0.002

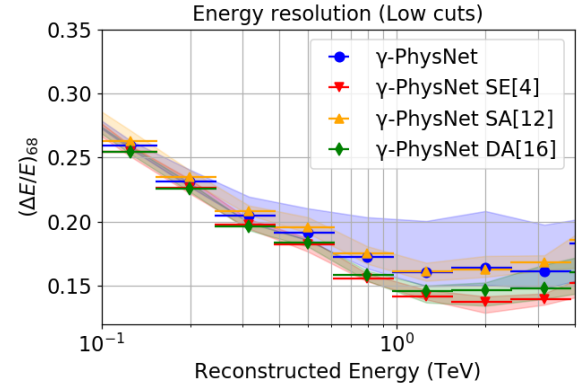


Figure 8: Low cuts. Energy resolution curves of the different attention mechanisms for γ -PhysNet. The surface represents the min / max envelope per bin and the dots represent the average resolution per bin of the six seeds.

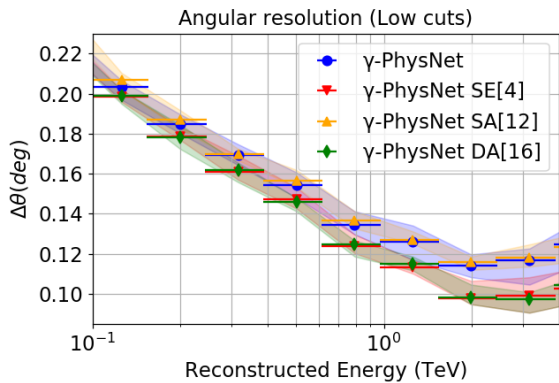


Figure 9: Low cuts. Angular resolution curves of the different attention mechanisms for γ -PhysNet. The surface represents the min / max envelope per bin and the dots represent the average resolution per bin of the six seeds.

5 DISCUSSION

5.0.1 Contribution of Multi-Task Learning to Gamma Astronomy

The comparison between γ -PhysNet and the widespread Hillas + RF method presented in Section 4.4 shows that neural networks, in particular MTL, dramatically improve the performance of IACT data analysis. Improvements in energy resolution will allow producing more detailed spectra, bringing more constraints on sources modeling. Improving the angular resolution and the classification will both improve the signal-to-noise ratio, thus allowing the detection of fainter sources in a significant way. Studies of extended sources at very high energies are quite recent. However, the studies made by H.E.S.S. show extended emissions corresponding to angular separation going from 0.05 degrees (corresponding to H.E.S.S. angular resolution) (Aharonian et al., 2019) to 0.3° (Hoppe et al., 2009). These values show that the gains obtained in angular resolution, even compared to the single task ResNet-56 (up to 0.08°), could make the difference between observing a point source and an extended source. This then allows for morphological studies, bringing important insights on the physics of these sources. Further, γ -PhysNet’s results are consistent with ImPACT (Parsons et al., 2016), a template-based method, and 500 times faster.

5.0.2 Contribution of Attention

The principal lesson of the study on attention methods for γ -PhysNet presented in Section 4.5 is that all attention methods help to reduce the variability of the results and thus to improve the robustness of the models. Another interesting insight is

that the self-attention mechanism, although the more complex, constantly underperforms. On the other hand, Squeeze-and-Excitation and dual attention significantly improve both energy and direction reconstruction task performance compared to γ -PhysNet without attention.

5.0.3 Real Data Discrepancy

Although we have high quality simulations to train γ -PhysNet, real data will certainly differ from simulated data. In (Shilon et al., 2019) Shilon *et al.* have shown that for H.E.S.S., the angular resolution was significantly degraded when a CNN was applied to real data, with a loss of about 0.04° compared to simulated data. In future work, we plan to use real data as soon as they are available to improve the performance of our architecture. Since ground truth is difficult to obtain from real data, GAN approaches could help to build up relevant feature representations of the real data. It has been successfully applied to light curve analysis in (Pasquet et al., 2019). Moreover, a phase of improvement of the simulation will be conducted when real data are available. We expect our model to benefit from the updated simulation.

6 CONCLUSION

In this paper we have presented γ -PhysNet, a physically inspired deep multi-task architecture for single telescope IACT full event reconstruction. Our model exploits the multi-task nature of IACT events to perform gamma / proton classification, energy and arrival direction reconstruction, outperforming the widespread Hillas + Random Forest analysis on Monte Carlo simulated data. Our extensive experiments show that MTL in the context of CTA data analysis achieves better performance than single task networks. We have then realized a study on attention mechanisms with two different selection cuts to address relevant use cases. Our experiments show that attention improves the performance and the robustness on energy and direction regression tasks.

The contribution of our multi-task architecture also lies in its speed as a substantial gain is expected by using a single network instead of one for each of the three tasks. Speed is actually a strong requirement to enable real-time source and transient event detection as well as alert broadcasting to other observatories.

ACKNOWLEDGEMENTS

We gratefully acknowledge financial support from the agencies and organizations listed here: www.cta-observatory.org/consortium_acknowledgment. This project has received funding from the *European Union's Horizon 2020 research and innovation programme* under grant agreement No 653477, and from the Fondation Université Savoie Mont Blanc. This work has been done thanks to the facilities offered by the Univ. Savoie Mont Blanc - CNRS/IN2P3 MUST computing center and HPC resources from GENCI-IDRIS (Grant 2020-AD011011577) and computing and data processing resources from the CNRS/IN2P3 Computing Center (Lyon - France). We gratefully acknowledge the support of the NVIDIA Corporation with the donation of one NVIDIA P6000 GPU for this research.

REFERENCES

- Abdalla, H., Adam, R., Aharonian, F., et al. (2019). A very-high-energy component deep in the γ -ray burst afterglow. *Nature*, 575(7783):464–467.
- Aharonian, F., Ait, B. F., Bernlöhr, K., Bordas, P., Casanova, S., Chakraborty, N., Deil, C., Donath, A., Hahn, J., Hermann, G., et al. (2019). Resolving the crab pulsar wind nebula at teraelectronvolt energies. *Nature Astronomy*.
- Ambrosi, G., Awane, Y., Baba, H., et al. (2013). The Cherenkov Telescope Array Large Size Telescope. *Proceedings of the 33rd International Cosmic Ray Conference*, pages 8–11.
- Bahdanau, D., Cho, K., and Bengio, Y. (2015). Neural machine translation by jointly learning to align and translate. In Bengio, Y. and LeCun, Y., editors, *3rd International Conference on Learning Representations, ICLR 2015, San Diego, CA, USA, May 7-9, 2015, Conference Track Proceedings*.
- Brunel, A., Pasquet, J., PASQUET, J., Rodriguez, N., Comby, F., Fouchez, D., and Chaumont, M. (2019). A cnn adapted to time series for the classification of supernovae. *Electronic Imaging*, 2019(14):90–1.
- Cao, J., Li, Y., and Zhang, Z. (2018). Partially shared multi-task convolutional neural network with local constraint for face attribute learning. In *Proceedings of the IEEE Conference on Computer Vision and Pattern Recognition*, pages 4290–4299.
- Caruana, R. (1997). Multitask learning. *Machine learning*, 28(1):41–75.
- Chen, Z., Badrinarayanan, V., Lee, C.-Y., and Rabinovich, A. (2018). GradNorm: Gradient normalization for adaptive loss balancing in deep multitask networks. In Dy, J. and Krause, A., editors, *Proceedings of the 35th International Conference on Machine Learning*, volume 80 of *Proceedings of Machine Learning Research*, pages 794–803. PMLR.
- de Naurois, M. and Rolland, L. (2009). A high performance likelihood reconstruction of γ -rays for imaging atmospheric Cherenkov telescopes. *Astroparticle Physics*, 32(5):231–252.
- Feng, Q., Lin, T. T., Collaboration, V., et al. (2016). The analysis of veritas muon images using convolutional neural networks. *Proceedings of the International Astronomical Union*, 12(S325):173–179.
- Fiasson, A., Dubois, F., Lamanna, G., Masbou, J., and Rosier-Lees, S. (2010). Optimization of multivariate analysis for IACT stereoscopic systems. *Astroparticle Physics*, 34.
- Guo, M., Haque, A., Huang, D.-A., Yeung, S., and Fei-Fei, L. (2018). Dynamic task prioritization for multitask learning. In *Proceedings of the European Conference on Computer Vision (ECCV)*, pages 270–287.
- He, K., Gkioxari, G., Dollar, P., and Girshick, R. (2017). Mask R-CNN. In *Proceedings of the IEEE International Conference on Computer Vision (2017)*.
- He, K., Zhang, J., Ren, S., and Sun, J. (2016a). Identity mappings in deep residual networks. In *European conference on computer vision*, pages 630–645. Springer.
- He, K., Zhang, X., Ren, S., and Sun, J. (2016b). Deep residual learning for image recognition. In *Proceedings of the IEEE conference on computer vision and pattern recognition*, pages 770–778.
- Hillas, A. (1985). Cerenkov light images of eas produced by primary gamma. In *International Cosmic Ray Conference*, volume 3.
- Hoppe, S. et al. (2009). Detection of very-high-energy gamma-ray emission from the vicinity of PSR B1706-44 with H.E.S.S. *arXiv e-prints*, page arXiv:0906.5574.
- Hu, J., Shen, L., and Sun, G. (2018). Squeeze-and-excitation networks. In *Proceedings of the IEEE conference on computer vision and pattern recognition*, pages 7132–7141.
- Iizuka, S., Simo-Serra, E., and Ishikawa, H. (2016). Let there be color! joint end-to-end learning of global and local image priors for automatic image colorization with simultaneous classification. *ACM Transactions on Graphics (ToG)*, 35(4):1–11.
- Jacquemont, M., Antiga, L., Vuillaume, T., Silvestri, G., Benoit, A., Lambert, P., and Maurin, G. (2019). Indexed operations for non-rectangular lattices applied to convolutional neural networks. In *Proceedings of the 14th International Joint Conference on Computer Vision, Imaging and Computer Graphics Theory and Applications - Volume 5: VISAPP*, pages 362–371. INSTICC, SciTePress.
- Kendall, A., Gal, Y., and Cipolla, R. (2018). Multi-task learning using uncertainty to weigh losses for scene geometry and semantics. In *Proceedings of the IEEE Conference on Computer Vision and Pattern Recognition*, pages 7482–7491.
- Kim, B., Brill, A., Miener, T., Nieto, D., and Feng, Q. (2019). DL1-Data-Handler: DL1 HDF5 writer, reader, and processor for IACT data. <https://doi.org/10.5281/zenodo.3336561>. v0.8.1-legacy.

- Kim, E. J. and Brunner, R. J. (2016). Star-galaxy classification using deep convolutional neural networks. *Monthly Notices of the Royal Astronomical Society*, page stw2672.
- Kingma, D. P. and Ba, J. (2015). Adam: A method for stochastic optimization. In Bengio, Y. and LeCun, Y., editors, *3rd International Conference on Learning Representations, ICLR 2015, San Diego, CA, USA, May 7-9, 2015, Conference Track Proceedings*.
- Luvizon, D. C., Picard, D., and Tabia, H. (2018). 2d/3d pose estimation and action recognition using multitask deep learning. In *Proceedings of the IEEE Conference on Computer Vision and Pattern Recognition*.
- Mangano, S., Delgado, C., Bernardos, M. I., et al. (2018). Extracting gamma-ray information from images with convolutional neural network methods on simulated cherenkov telescope array data. In *IAPR Workshop on Artificial Neural Networks in Pattern Recognition*, pages 243–254. Springer.
- Nieto, D., Brill, A., Feng, Q., Jacquemont, M., Kim, B., Miener, T., and Vuillaume, T. (2019). Studying deep convolutional neural networks with hexagonal lattices for imaging atmospheric cherenkov telescope event reconstruction. In *ICRC 2019 - 36th International Cosmic Ray Conference*.
- Nieto, D., Brill, A., Kim, B., et al. (2017). Exploring deep learning as an event classification method for the Cherenkov Telescope Array. *arXiv preprint arXiv:1709.05889*, pages 1–8.
- Parmar, N., Ramachandran, P., Vaswani, A., Bello, I., Levskaya, A., and Shlens, J. (2019). Stand-alone self-attention in vision models. In *Advances in Neural Information Processing Systems*, pages 68–80.
- Parmar, N., Vaswani, A., Uszkoreit, J., Kaiser, L., Shazeer, N., Ku, A., and Tran, D. (2018). Image transformer. In Dy, J. and Krause, A., editors, *Proceedings of the 35th International Conference on Machine Learning*, volume 80 of *Proceedings of Machine Learning Research*, pages 4055–4064. PMLR.
- Parsons, R., Murach, T., and Gajdus, M. (2016). Hess ii data analysis with impact. In *The 34th International Cosmic Ray Conference*, volume 236, page 826. SISSA Medialab.
- Parsons, R. and Ohm, S. (2019). Background rejection in atmospheric cherenkov telescopes using recurrent convolutional neural networks. *arXiv preprint arXiv:1910.09435*.
- Pasquet, J., Pasquet, J., Chaumont, M., and Fouchez, D. (2019). Pelican: deep architecture for the light curve analysis. *Astronomy & Astrophysics*, 627:A21.
- Pavlo, D., Feichtenhofer, C., Grangier, D., and Auli, M. (2019). 3d human pose estimation in video with temporal convolutions and semi-supervised training. In *Proceedings of the IEEE Conference on Computer Vision and Pattern Recognition*, pages 7753–7762.
- Pedregosa, F., Varoquaux, G., Gramfort, A., Michel, V., Thirion, B., Grisel, O., Blondel, M., Prettenhofer, P., Weiss, R., Dubourg, V., Vanderplas, J., Passos, A., Cournapeau, D., Brucher, M., Perrot, M., and Duchesnay, E. (2011). Scikit-learn: Machine learning in Python. *Journal of Machine Learning Research*, 12.
- Ren, Z. and Jae Lee, Y. (2018). Cross-domain self-supervised multi-task feature learning using synthetic imagery. In *Proceedings of the IEEE Conference on Computer Vision and Pattern Recognition*, pages 762–771.
- Ruder, S. (2017). An overview of multi-task learning in deep neural networks. *arXiv preprint arXiv:1706.05098*.
- Sener, O. and Koltun, V. (2018). Multi-task learning as multi-objective optimization. In *Advances in Neural Information Processing Systems*.
- Shilon, I., Kraus, M., Büchele, M., Egberts, K., Fischer, T., Holch, T. L., Lohse, T., Schwanke, U., Steppa, C., and Funk, S. (2019). Application of deep learning methods to analysis of imaging atmospheric cherenkov telescopes data. *Astroparticle Physics*, 105:44–53.
- Sun, J., Darbeha, F., Zaidi, M., and Wang, B. (2020). Saunet: Shape attentive u-net for interpretable medical image segmentation. *arXiv preprint arXiv:2001.07645*.
- Thrun, S. (1996). Is learning the n-th thing any easier than learning the first? In *Advances in neural information processing systems*, pages 640–646.
- Touvron, H., Vedaldi, A., Douze, M., and Jégou, H. (2019). Fixing the train-test resolution discrepancy. In *Advances in Neural Information Processing Systems*, pages 8252–8262.
- Vaswani, A., Shazeer, N., Parmar, N., Uszkoreit, J., Jones, L., Gomez, A. N., Kaiser, Ł., and Polosukhin, I. (2017). Attention is all you need. In *Advances in neural information processing systems*, pages 5998–6008.
- Völk, H. J. and Bernlöhr, K. (2009). Imaging very high energy gamma-ray telescopes. *Experimental Astronomy*, 25(1-3).
- Wang, X., Girshick, R., Gupta, A., and He, K. (2018). Non-local neural networks. In *Proceedings of the IEEE conference on computer vision and pattern recognition*, pages 7794–7803.
- Yuan, Y., Chen, X., and Wang, J. (2020). Object-contextual representations for semantic segmentation. In *Computer Vision – ECCV 2020*.
- Zhang, H., Goodfellow, I., Metaxas, D., and Odena, A. (2019). Self-attention generative adversarial networks. In *International Conference on Machine Learning*, pages 7354–7363.
- Zhang, H., Wu, C., Zhang, Z., et al. (2020). Resnest: Split-attention networks. *arXiv preprint arXiv:2004.08955*.